Hydrogen Bonding in the Indole−Water Complex: A High Resolution UV Study of the Hydrogen Donor Conformer

R. M. Helm, M. Clara, Th. L. Grebner,† and H. J. Neusser*

Institut für Physikalische und Theoretische Chemie, Technische Universität München, Lichtenbergstrasse 4, 85748 Garching, Germany

Received: December 30, 1997; In Final Form: February 26, 1998

The nature of the intermolecular bonding in the indole−water complex is investigated by highly resolved UV-REMPI spectra with rotational fine structure. First, we determine the coordinates of the amino hydrogen atom by isotope substituting it with deuterium for the S_0 electronic ground and S_1 excited state of indole. In a second step, we calculate the rotational fine structure resulting from possible cluster structures and compare it with the experimental results. A fit routine adapts the spectroscopic constants within the condition of a planar complex which is a reasonable assumption for the observed rotational a,b-type band structure. The best agreement between simulation and experiment is found when the water molecule oxygen is located 2.93(5) Å away from the amino hydrogen of indole. This clearly demonstrates that in the indole−water complex a hydrogen bond is formed between the hydrogen donor indole and the oxygen atom of the water molecule. Upon electronic excitation to S_1 this bond length is nearly constant.

I. Introduction

The indole (C_8H_7N) chromophore of the amino acid tryptophan has been subject of extensive spectroscopic studies.[1−10] Due to its chemical stability and long S_1 lifetime, indole is suitable for UV spectroscopy and serves as a model system for investigation of the photochemistry of the amino acids. It is responsible for the UV protein absorption and fluorescence. Its hydrogen bonding is important for the understanding of solvation processes in chemistry and the stability and structure of biological systems in natural surrounding.

There is a wide literature on the spectroscopy of the indole monomer. In the gas phase the structure was determined by spectroscopic techniques such as microwave (MW),[5] dispersed fluorescence (DF),[2] vibrationally resolved[6−8] laser induced fluorescence spectroscopy (LIF), rotational contour LIF,[1] and rotationally resolved LIF.[9] Only few UV rotationally resolved spectra of hydrogen-bonded aromatic molecule−water complexes have been recorded (i.e. refs. 11−14). This is due to the low symmetry of these complexes and the resulting complicated rotational analysis. The indole−water cluster was investigated by vibrationally resolved LIF spectroscopy and resonance enhanced multiphoton ionization (REMPI).[3,4] Yet no structural information is available particularly due to the lack of a microwave spectrum. Thus, the position of the water attached to the indole is still under discussion.

Two different conformers of the hydrogen-bonded indole−water complex were postulated in ref 2 with the water molecule acting as a hydrogen acceptor or as a hydrogen donor. There has been some discussion on the structure of these isomers but no direct experimental data is available on that point. The intensity of the band postulated as originating from the solvent hydrogen acceptor (^1L_b) conformer is much larger in the measured spectra than the other origin (^1L_a). The energetics of the binding in the most abundant conformer is investigated in our accompanying work.[10] There, for the first time a precise value for the binding energy of the hydrogen-bonded water in the neutral and ionic complex is presented. Here, we address the question concerning its structure.

We present highly resolved REMPI spectra of the hydrogen-bonded aromatic molecule−water system indole−water. This was feasible by application of the mass-selective REMPI-technique. It consists of the combination of Fourier-transform limited narrow band laser pulses for excitation, ionization with broad band laser pulses, and mass-selective detection of the ions. The structure is determined in two steps. The position of the amino hydrogen atom is determined by the analysis of the isotope substituted indole-d_1 $S_1 \leftarrow S_0$ spectrum. The position of the water molecule is determined by the analysis of the indole−water $S_1 \leftarrow S_0$ spectrum. From a combination of both results the bond length is calculated.

II. Experimental Section

For production of indole−water complexes Ar gas at a backing pressure of 5 bar was mixed with water vapor of 5 mbar. The gas mixture was expanded from a heated (110 °C) reservoir of indole through a pulsed valve (modified Bosch) with a 200 μm orifice leading to a supersonic beam and the production of complexes of indole with water. Deuterated indole-d_1 was produced by solvating indole in deuterated sulforic acid and separating the deuterated indole several times. The experimental apparatus for the recording of high resolution UV spectra by mass-selected resonance-enhanced two-photon ionization was described in detail in our previous work.[15] Briefly, the light of an Ar^+-laser (Spectra Physics 171) pumps a continuous wavelength (cw) single-mode ring dye laser (Coherent CR 699/29, rhodamine 6G). Its output is pulsed amplified in three amplifier stages operating with the dyes coumarine 153/rhodamine 6G and pumped by a XeCl excimer laser (Lambda Physik MSC 201). After the frequency of the visible light, was doubled the UV pulses have a duration of 10 ns (fwhm) and are attenuated to a pulse energy of 0.02 mJ. Their frequency

† Present address: Labor für Organische Chemie, ETH-Zürich, Universitätsstr. 16, 8092 Zürich, Switzerland.

S1089-5639(98)00597-0 CCC: $15.00
Published on Web 04/22/1998

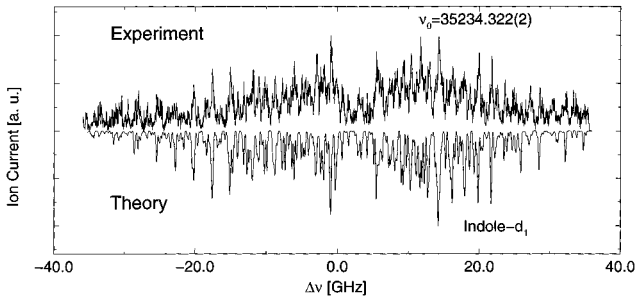

Figure 1. Upright trace: Highly resolved UV spectrum of indole-d_1: $S_1 \leftarrow S_0, 0_0^0$ transition measured by mass-selected resonance-enhanced two-photon ionization. Inverted trace: Calculated spectrum using the rotational constants found by the CARF method as described in the text.

width is 60 MHz (fwhm), which is close to the Fourier transform limit. For ionization, the light of a XeCl excimer laser-pumped broad-band dye laser (Lambda-Physik FL 2002, RDC360neu) was directed perpendicularly to the molecular beam counter-propagating the excitation laser beam. The light pulses of the ionization laser have an energy of 6 mJ and a duration of 10 ns (fwhm).

The mass-selective detection is performed by a home-built linear time of flight mass spectrometer. A gated boxcar integrator (Stanford Research Systems SR250) integrates the signal of the channel plates in the appropriate time window. A microcomputer (Force CPU-37) controls the laser frequency and records the signal intensity and the calibration signals.

The relative frequency calibration signal during the laser scan is provided by the transmission spectrum of the visible cw laser light through a Fabry−Perot interferometer with 150 MHz free spectral range. The simultaneous measured iodine vapor fluorescence excitation spectrum allows us to calibrate the absolute frequency.[16,17]

III. Results and Discussion

A. Indole. *1. Spectrum of Monodeuterated Indole.* To determine the position of the amino hydrogen in indole, we measured the spectrum of indole-d_1 (C_8H_6ND). In Figure 1 (upper trace), the ion current between $\nu_1 = 35233.1$ cm^{-1} and 35235.5 cm^{-1} recorded at mass of 118 u, the mass of indole-d_1, is plotted. The ionization laser frequency ν_2 was fixed to 28169 cm^{-1}. The experimental spectrum has two broad wings with a hole in the center, as is typical for a mostly a- and b-type transition with a P- and R-branch and a missing Q-branch.

The first step of the analysis is a simulation of the rotational structure of the band. The ground-state rotational constants A'', B'', C'' of indole-d_1 are known from microwave experiments.[5] We used a rigid asymmetric rotor model[18] to calculate the spectrum. The free parameters, the three excited state rotational constants A', B', C', and the transition energy are determined in the fit routine. Line width, line shape, orientation of the transition dipole moment, and rotational temperature are fixed to reasonable values and adapted by hand afterwards.

For the simulation we used the recently developed algorithm of correlation automated rotational fitting (CARF)[19] based on a crosscorrelation between experiment and simulation. The quality of a fit is given by the height of the crosscorrelation peak. Its position defines the relative position of the experimental and simulated spectrum and therefore the band origin. The height of the cross-correlation peak is optimized sequentially in a fit procedure.

We started the CARF procedure with the rotational constants of the monodeuterated indole ground state[5] and S_1 starting values

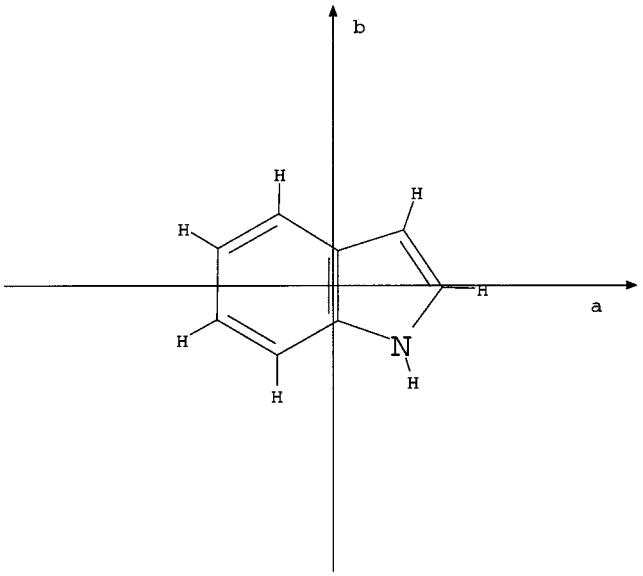

Figure 2. Structure and principle axes definition of the indole monomer.

TABLE 1: Rotational Constants of Indole and Indole-d_1

	indole[a]	indole-d_1
A''[MHz][b]	3877.828(6)	3762.06(3)
B''[MHz][b]	1636.047(1)	1617.453(4)
C''[MHz][b]	1150.8997(8)	1131.454(5)
$\Delta I''$[amu Å^2]	−0.1113(7)	−0.126(3)
A'[MHz]	3743.077(8)	3627.7(30)
B'[MHz]	1618.13(4)	1600.0(14)
C'[MHz]	1130.17(1)	1110.9(13)
$\Delta I'$[amu Å^2]	−0.168(8)	−0.25(61)
E_0[cm^{-1}]	35231.420(6)	35234.322(2)

[a] From ref 9. [b] From ref 5.

calculated from the S_0 structure[5] and the S_1 protonated indole rotational constants.[9] The spectrum yielding the best cross-correlation is shown in the lower inverted trace of Figure 1. The a- to b-type ratio was set to 1:1, meaning a transition moment oriented at 45° with respect to the principal *a*- and *b*-axis of indole-d_1 (see Figure 2 for illustration of the axes) in the plane of indole-d_1. The rotational temperature for the simulation was chosen 2 K. The simulated stick spectrum was convoluted with a Gaussian line shape of 150 MHz line width, representing the overall experimental resolution. This line width is mostly caused by the laser line width of 70 MHz, the Doppler broadening of 30 MHz, and the natural line width of roughly 20 MHz.[9]

The experimental line positions agree quite nicely with the respective positions in the theoretical spectrum. The agreement of the experimental and theoretical line intensities is satisfactory with stronger deviations in the wings on both sides of the spectrum. Using different rotational temperatures and Voigt line shapes would increase the visual agreement between theory and experiment, but not improve the quality of the rotational constants. The rotational constants found by this procedure are summarized together with the respective values for the protonated indole[9] and the ground state[5] in Table 1.

2. Indole Structure. Now, the rotational constants of indole and indole-d_1 are available for the S_0 and the S_1 state. Next we calculate the position of the amino hydrogen in both electronic states using the Kraitchman's equations (ref 20, eq 1) for monosubstitution. For symmetry reasons the planarity of the molecule is presumed. $I_{x,y,z}$ are the inertial moments of the unsubstituted molecule, $I'_{x,y,z}$ the inertial moments of the

TABLE 2: Coordinates of the Substituted Amino Hydrogen in the CM-System of Protonated Indole

	S_0[a]	S_1
x[Å]	2.0250(3)	2.095(1)
y[Å]	0.0	0.0
z[Å]	1.865(3)	1.861(6)

[a] From ref 5.

substituted molecule, and μ is the reduced mass.

$$x = \sqrt{\frac{(I'_x - I_z)\,(I'_z - I_z)}{(I_x - I_z)\,\mu}} \qquad y = 0$$
$$z = \sqrt{\frac{(I'_z - I_x)\,(I'_x - I_x)}{(I_z - I_x)\,\mu}} \tag{1}$$

The result is shown in Table 2. The coordinates are given in the inertial system of protonated indole and the error is determined by the Gaussian law of error propagation. This error is based on the notion of a rigid structure and does not include vibrational averaging effects. The distance of the amino hydrogen from the center of mass changes slightly from S_0 to S_1. This can be explained by the change of the ring structure after electronic excitation. Now the position of the nitrogen's H-atom is known and we are able to determine its distance from the docking water molecule, (i.e., the length of the hydrogen bond).

B. Indole−Water. *1. Spectra.* In Figure 3 (upper trace) the ion current at the mass of indole−water (135 u) between $\nu_1 = 35098.3$ cm^{-1} and 35100.4 cm^{-1} is plotted. The ionization laser frequency ν_2 was fixed at 27397 cm^{-1}. Similar to the monomer spectrum, the cluster spectrum has two broad wings with a hole in the center, as is typical for a mostly a- and/or b-type transition. From this it is clear that the main inertial $a-b$ plane does not change upon attachment of the H_2O molecule i.e., (the center of mass of the water molecule is located in the plane of indole and not above the plane of indole, such as in the case of benzene−water[21]).

The detailed analysis of this band is far more complicated than in the monomer spectrum since neither rotational constants in either electronic states nor the orientation of the dipole transition moment are available for the cluster. A CARF fit of all 12 parameters (6 rotational constants, 2 projections of the transition dipole moment on the inertial axes, electronic origin, rotational temperature, line shape, and line width) was not possible since the dimension of the problem is too large and the fit parameters A', B', C', and A'', B'', C'' are not independent of each other. The best fits define a hyper plane in which fits of similar quality for different pairs of constants are located. Therefore we proceeded in an alternative way: Assuming planarity of the cluster to reduce the number of free parameters, we adapted A', B', A'', and B'' in the fit routine. C' and C'' are calculated by the planarity conditions ($1/C' = 1/A' + 1/B'$ and $1/C'' = 1/A'' + 1/B''$, respectively). The rotational temperature, the line width and the line shape are not taken as fit parameters but are fixed to reasonable values during the automatic fit procedures. To gain starting values for this procedure, we assumed various structures of the indole−water complex for a position of water with fixed internal structure[22] relative to the fixed internal structure of indole[9] in S_0 and S_1, respectively. From the assumed special cluster structure we calculated the inertial tensor of the complex by transforming the inertial tensor of the water molecule to a representation in the indole center of mass coordinate representation and by summation according

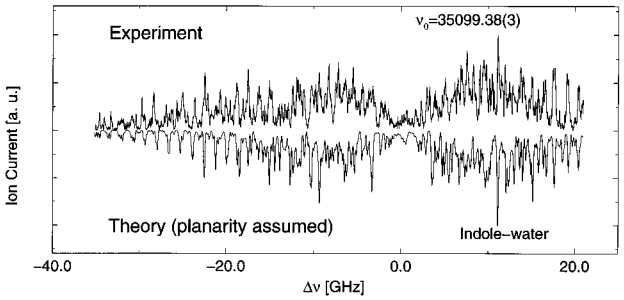

Figure 3. Upright trace: Highly resolved UV spectrum of indole−water: $S_1 \leftarrow S_0,0_0^0$ transition measured by mass-selected resonance-enhanced two-photon ionization. Inverted trace: Calculated spectrum using the rotational constants found by the CARF method (see Figure 4).

Steiner's law (ref 23, eq 2).

$$I_{xx}^{Cl} = I_{xx}^{Mo} + m^{Mo}(y'^2 + z'^2) + \sum_{i=1}^{3} m_i[(y_i - y')^2 + (z_i - z')^2]$$

$$I_{xy}^{Cl} = -\sum_{i=1}^{3} m_i x_i y_i + m^{Cl} x' y' \qquad \text{with}$$
$$x' = \frac{1}{m^{Cl}}\sum_{i=1}^{3} m_i x_i \qquad y' = \frac{1}{m^{Cl}}\sum_{i=1}^{3} m_i y_i \qquad z' = \frac{1}{m^{Cl}}\sum_{i=1}^{3} m_i z_i \tag{2}$$

All coordinates are in the principal system of the monomer, the superscripts Mo and Cl are the respective quantities of the monomer (indole) and the cluster (indole−water). The index i concerns the three water atoms with the masses m_i and the coordinates (x_i, y_i, z_i). With cyclic permutation of the indices the other components of the inertial tensor are calculated. Its diagonalization yields the rotational constants for the assumed structure. The error is determined by the Gaussian law of error propagation. A necessary assumption for the application of eqs 1 and 2 is the notion of a rigid structure and therefore underestimates the actual errors. The need for this precaution is indicated by the results from our accompanying work[10] where low-frequency intermolecular vibrations of indole−water are reported. The low frequencies indicate that large amplitude motions are present, which will significantly increase the errors and lead to average bond lengths.

The type of transition moment in the cluster arises from the new orientation of the S_0 inertial axes in respect to the dipole transition moment of the indole monomer. Here we have assumed that the orientation of the transition moment in indole is not affected by complexation. The new transition dipole moment orientation is rotated by the angle θ (eq 3) within the $x-z$ ($a-b$) Plane due to the assumed planarity of the cluster.

$$\theta = {}^1/_2 \arctan \frac{2I_{xz}}{I_{xx} - I_{zz}} \tag{3}$$

For every assumed structure, nine parameters are calculated: three S_0 ground rotational constants A'', B'', C'', three S_1 excited state rotational constants A', B', C' and the three projections of the cluster inertial axes on the indole dipole transition moment. Assuming with reasonable values for the rotational temperature, the line width and the line shape, the respective $S_1 \leftarrow S_0$ spectrum is calculated. A least-squares algorithm combined with the cross-correlation analysis yields the quality of the simulation and adapts the rotational constants within the

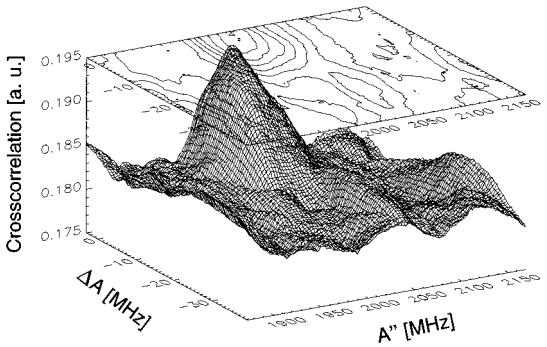

Figure 4. Two-dimensional maximum of the crosscorrelation between the experimental and theoretical cluster spectrum shown in Figure 3 as a function of A'' and ΔA. The contour lines represent positions with equal correlation. The strong central peak yields the rotational constants for the best fit of the experimental spectrum.

TABLE 3: Rotational Constants of the Indole−Water Donor Confomer Obtained in this Work with the CARF Method and the Condition of a Planar Cluster

A''[MHz]	2022(10)
B''[MHz]	736(7)
C''[MHz]	540(5)
$\Delta I''$[amu Å^2]	0 (condition)
A'[MHz]	2024(10)
B'[MHz]	727(7)
C'[MHz]	535(5)
$\Delta I'$[amu Å^2]	0 (condition)
E_0[cm^{-1}]	35099.38(3)

condition of a planar complex ($1/C = 1/A + 1/B$). The origin ν_0 is given by the position of the maximum of the cross-correlation between theory and experiment. Figure 4 illustrates the result of the cross-correlation procedure. It shows a two dimensional grid scan of the relative magnitude of the cross-correlation as a function of the rotational constants A'' and $\Delta A = A'' - A'$ around the maximum. There is a dominating peak which ensures that there is a clear assignment of the rotational constants and no side maximum. Outside the plotted range of Figure 4 the cross correlation decreases to lower values. The rotational constants used to simulate the spectrum in Figure 3 are listed in Table 3. For the simulation a Gaussian line shape was assumed and the line width was set to 150 MHz. The rotational temperature was chosen and fixed to 3.0 K and the orientation of the dipole transition moment was set nearly parallel to the *b*-axis of the cluster with 5% *a*-contribution. The best agreement between experimental and simulated spectrum achieved with this planar contour fit procedure is shown in the lower inverted trace of Figure 3. The agreement of line positions is quite satisfactory regarding the assumptions made for this planar CARF procedure. On the basis of our experimental data, we can neither conclude whether there exists a small inertial defect nor a rotational line splitting within the large error bars.

2. Structure. We performed structure calculations to determine the bond length. The distances and the angular orientation of the torsional tensors of indole and water were varied in order to reproduce the measured rotational constants best. A conjugate gradient algorithm minimizes the sum of the squares of the differences of measured and calculated (eq 2) rotational constants. From this procedure the absolute values of the *x*- and ***z***-coordinate of the water in the principal system of the indole monomer are known. Since the water is assumed to be located in the plane of indole, the absolute value of the *y*-coordinate is zero and four possible structures remain ($\pm x$, 0, $\pm z$). Besides the two nearly equivalent positions at the benzene ring ($-x$, 0, $\pm z$), the position at the amino hydrogen ($+x$, 0, $-z$), and the position on the opposite side of the amino hydrogen ($+x$, 0, $+z$) remain (see Figure 2). The two nearly equivalent positions at the benzene ring can be excluded since none of the two structures should be preferred and this position should result in two similar bands located close to each other. There is only one spectrum observed. From the two remaining possible positions we favor the docking position at the amino hydrogen due to the electronegativity of the nitrogen atom (see Figure 5).

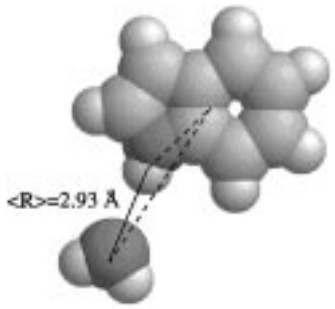

Figure 5. Experimentally found structure of the hydrogen bonded indole−water complex. The coordinates of the amino hydrogen in the principal system of indole is determined by the high resolution UV experiments of indole-d_1 in the first part of this work (dashed line). The position of the waters center of mass (CM) in respect to the cluster CM in the second part (dashed line) is found by the CARF method with the assumption of a planar cluster. The difference of both is the bond length $\langle R \rangle$ (solid line).

TABLE 4: Average Bond Length of the Indole−Water Cluster in Its S_0 and S_1 Electronic State

	$\langle R \rangle$[Å]
S_0	2.935(50)
S_1	2.934(50)

With the known position of the amino hydrogen in the respective electronic states (see section III.A.2) the result is transformed to a new representation. The H−O bond distance between the amino hydrogen of indole is $\langle R \rangle$ and the oxygen of the water is orientated towards the amino hydrogen as illustrated in Figure 5. The resulting bonding characteristics for S_0 and S_1 are summarized in Table 4.

Comparing our results for indole−water with the ones of other investigated hydrogen bonded aromatic molecule−water systems, we can distinguish two types of hydrogen bonds, the single- and double-bonded systems: In benzonitrile−water[12] and pyridone−water,[13] the water is doubly bonded with two different bond length. In phenol−water the character of the bond is that of a single bond and is similar to the present situation in indole−water. However, the oxygen atom of the phenol forms a stronger hydrogen bond than the nitrogen atom of the indole. This can be seen from the shorter bond length in phenol−water in S_0 (S_1) of roughly 1.97 Å (1.93 Å)[11,24] with respect to indole−water of S_0 (S_1) of 2.935(50) Å (2.933(50) Å). In the accompanying paper,[10] we show that the binding energy of the indole−water complex is smaller than the binding energy of water to the OH group in naphthol−water.[25] From this comparison, we may expect that also the binding of water to the OH group in phenol−water is larger than to the NH group in indole−water, which is in line with the longer bond length of the latter found in this work.

IV. Summary and Conclusion

In this work we present highly resolved UV-REMPI spectra with rotational fine structure of indole-d_1 and the hydrogen

bonded indole−water complex. The structural information about the hydrogen bond is achieved in two steps. First, we measure and calculate the $S_1 \leftarrow S_0$ spectrum of indole-d_1. From the so-obtained rotational constants, the position of the amino hydrogen atom is determined for the electronic ground and excited state. Secondly, we measure and simulate the $S_1 \leftarrow S_0$ spectrum of indole−water. On the basis of possible cluster structures, spectra are calculated and the resulting rotational spectra compared with the experimental results. Afterward a fit routine adapts the rotational constants within the condition of a planar cluster which is a reasonable assumption for the observed a,b-type rotational band contour. The best agreement between calculated and experimental spectrum yields a structure with the water oxygen located 2.93(5) Å away from the amino hydrogen of indole. Upon electronic excitation to S_1, this bond length remains nearly constant.

When we compare the result found for indole−water with the single-bonded water in phenol−water, we find a weaker bonding with larger bond distance in case of the NH hydrogen donor functional group. This conclusion is supported by the experimental results of the binding energy presented in the accompanying work. As indole is the chromophore of tryptophan, all results for the indole−water complex are expected to provide a reliable basis for advanced calculations to gain a detailed knowledge on the potential energy surfaces of the hydrogen bonding process in amino acids.

Acknowledgment. Financial support from the Deutsche Forschungsgemeinschaft (Schwerpunkt "Molekulare Cluster") and the Fonds der Chemischen Industrie is gratefully acknowledged. We thank Dr. R. Neuhauser, J. Braun, and K. Siglow for helpful discussions and experimental support.

References and Notes

(1) Philips, A. L.; Levy, D. H. *J. Chem. Phys.* **1986**, *85*, 1327.
(2) Tubergen, M. J.; Levy, D. H. *J. Phys. Chem.* **1991**, *95*, 2175.
(3) Hager, J.; Ivanco, M.; Smith, M. A.; Wallace, S. C. *Chem. Phys.* **1986**, *105*, 397.
(4) Hager, J.; Ivanco, M.; Smith, M. A.; Wallace, S. C. *Chem. Phys. Lett.* **1985**, *113*, 503.
(5) Caminati, W.; di Bernando, S. *J. Mol. Struct.* **1990**, *253*.
(6) Outhouse, E. A.; Bickel, G. A.; Demmer, D. R.; Wallace, S. C. *J. Chem. Phys.* **1991**, *95*, 6261.
(7) Lipert, R. J.; Bermudez, G.; Colson, S. D. *J. Phys. Chem.* **1988**, *92*, 3801.
(8) Barstis, T. L. O.; Grace, L. I.; Dunn, T. M.; Lubman, D. M. *J. Phys. Chem.* **1993**, *97*, 5820.
(9) Berden, G.; Meerts, W. L.; Jalviste, E. *J. Chem. Phys.* **1995**, *103*, 9596.
(10) Braun, J. E.; Grebner, Th. L., Neusser, H. J. *J. Phys. Chem.* **1998**. xxxx
(11) Berden, G.; Meerts, W. L.; Schmitt, M.; Kleinermanns, K. *J. Chem. Phys.* **1996**, *104*, 972.
(12) Helm, R. M.; Vogel, H.-P.; Neusser, H. J.; Storm, V.; Consalvo, D.; Dreizler, H. *Z. Naturforsch.* **1997**, *52a*, 655.
(13) Held, A.; Pratt, D. W. *J. Am. Chem. Soc.* **1993**, *115*, 9708.
(14) Humphrey, S. J.; Pratt, D. W. *J. Chem. Phys.* **1996**, *104*, 8332.
(15) Sussmann, R; Neuhauser, R.; Neusser, H. J. *Can. J. Phys.* **1994**, *72*, 1179.
(16) Gerstenkorn, S.; Luc, P. *Atlas du spectre d'absorption de la molecule d'Iode*; Centre du National de la Recherche Scientifique (CNRS): Paris, 1978.
(17) Gerstenkorn, S.; Luc, P. *Rev. Phys. Appl.* **1979**, *14*, 791.
(18) Kroto, H. W. *Molecular Rotation Spectra*; Wiley and Sons: London, 1975.
(19) Helm, R. M.; Vogel, H.-P.; Neusser, H. J. *Chem. Phys. Lett.* **1997**, *270*, 285.
(20) Gordy, W.; Cook, R. L. *Microwave Molecular Spectra*; Wiley-Interscience: New York, 1984.
(21) Pribble, R. N.; Zwier, T. S. Faraday Discuss. **1994**, *97*, 229.
(22) Lucia, F. C.; Helminger, P.; Gordy, W. *Phys. Rev. A* **1973**, *8*, 2785.
(23) Landau, L. D.; Lifschitz, E. M. *Lehrbuch der theoretischen Physik I, Mechanik*; Akademie-Verlag: Berlin, 1976.
(24) Gerhards, M.; Schmitt, M.; Kleinermanns, K.; Stahl, W. *J. Chem. Phys.* **1996**, *104*, 967.
(25) Bürgi, T.; Droz, T.; Leutwyler, S. *Chem. Phys. Lett.* **1995**, *246*, 291.